Particuology 113 (2026) 180–188

Contents lists available at ScienceDirect

Particuology

journal homepage: www.elsevier.com/locate/partic

Assessment of the interplay between convective heat transfer and reaction kinetics during plastic pyrolysis

Feichi Zhang[a,*], Muhao Li[a], Xiaoyue Ma[a], Niklas Netsch[a], Salar Tavakkol[a,**], Thorsten Zirwes[b], Rui Zhang[c], Dieter Stapf[a]

[a] Institute for Technical Chemistry, Karlsruhe Institute of Technology, Kaiserstr.12, 76131, Karlsruhe, Germany
[b] Institute for Reactive Flows, University of Stuttgart, Pfaffenwaldring 31, 70569, Stuttgart, Germany
[c] Nanjing University of Science and Technology, Xiaolingwei Street, 210094, Nanjing, China

ARTICLE INFO

Keywords:
Plastic pyrolysis
Chemical recycling
Pyrolysis reaction
Heat transfer
Pyrolysis number

ABSTRACT

This work numerically investigates the pyrolysis of five common thermoplastics using a homogeneous, single-particle model (0D) to elucidate the interplay between convective heat transfer and reaction kinetics. The results reveal a fundamental competition between external heat supply and the endothermic cooling effect of the reaction, manifesting as a temperature plateau where heat input is balanced by the reaction enthalpy. We demonstrate that enhanced heat transfer—achieved via smaller particle sizes or higher Nusselt numbers—shifts the process toward higher reaction rates and temperatures. To quantify this behavior, we utilize the Pyrolysis number (*Py*), defined as the ratio of the characteristic chemical reaction time to the convective heat transfer time. A universal inverse correlation is identified between the dimensionless pyrolysis time and *Py*, valid across all investigated polymers and operating conditions. This correlation delineates two distinct operational regimes: reaction-limited control ($Py > 1$) and convective-heating limited control ($Py < 1$). These findings provide a predictive framework for optimizing heating rates and estimating residence times for complete conversion. Finally, comparison with particle-resolved (1D) simulations shows that neglecting intra-particle heat conduction causes faster heating and pyrolysis conversion, thereby underestimating the overall pyrolysis duration.

1. Introduction

Global plastic waste management remains critically deficient: of the approximately 400 Mt produced annually, only about 9% is recycled. The remainder is either mismanaged and released into the environment (22%) or disposed of through landfilling and incineration (69%), leading to substantial greenhouse gas emissions (Geyer et al., 2017). This recycling deficit is driven by the shortcomings of mechanical recycling, a process limited to pure, thermoplastic feedstocks that inevitably downgrades material quality (downcycling). In contrast, pyrolysis effectively reverses polymerization by thermally degrading plastic polymers at high temperatures under an inert atmosphere to produce valuable petrochemical feedstocks. A key advantage of this process is its tolerance for contaminated and mixed plastics, which are unsuitable for mechanical recycling. Consequently, pyrolysis is considered a promising technology to address the environmental challenges of end-of-life plastics by enabling feedstock recycling (Armenise, SyieLuing, et al., 2021; Kusenberg et al., 2022; Lopez et al., 2017). However, further development is required to improve its process design, product yields, energy efficiency, scalability, and economic viability (Ragaert et al., 2017).

For decades, thermogravimetric analysis (TGA) has been the foundation of research into plastic pyrolysis kinetics. Early studies focused on determining fundamental kinetic parameters for polymers like PE, PVC, and HDPE under various conditions (Bockhorn et al., 1999; Ceamanos et al., 2002). Later work revealed greater complexity, with studies on municipal waste demonstrating that decomposition requires multi-step reaction mechanisms rather than simple first-order models (Silvarrey & Phan, 2016). TGA has also been crucial for defining the operational temperature window for pyrolysis (typically 300 - 520 °C) and for ranking the thermal stability of different plastics (Das & Tiwari, 2017). Beyond TGA, research has advanced to reactor-scale investigations to understand

This article is part of a special issue entitled: Reactive Particle-Gas Systems II published in Particuology.

* Corresponding author.
** Corresponding author.
E-mail addresses: Feichi.Zhang@kit.edu (F. Zhang), salar.tavakkol@kit.edu (S. Tavakkol).

https://doi.org/10.1016/j.partic.2026.03.019
Received 30 November 2025; Received in revised form 17 February 2026; Accepted 8 March 2026
Available online 27 March 2026

process dynamics. Studies have focused on optimizing parameters, such as the work by López et al. (López et al., 2011), who identified optimal conditions for municipal plastic wastes at approximately 500 °C and residence times of 15–30 min in a semi-batch reactor, under which the highest yield and quality of pyrolysis liquids were obtained. The influence of heating rate and residence time on product yields was further clarified by Singh et al. (Singh et al., 2019) in a batch reactor. More advanced studies have focused on targeted product generation, for instance, using catalysis to maximize valuable olefin yields in an auger-type reactor (Netsch et al., 2023). Other critical factors have been identified, including the intrinsic polymer composition and morphology (Zeller et al., 2023) and the significant impact of high-pressure conditions on reaction pathways (Cheng et al., 2020; Wang et al., 2023). Crucially, the technology's industrial potential has been demonstrated in pilot-scale fluidized-bed reactors, validating its scalability (Kaminsky, 2021; Zhang, Tavakkol, et al., 2024).

Complementing experimental efforts, computational modeling has emerged as a powerful tool for investigating plastic pyrolysis. At the particle scale, models have successfully captured the complex physics of heating, melting, and pyrolysis for various plastics, with results validated against experimental data (Mazloum et al., 2021a, 2021b). The importance of particle-level characteristics was further underscored by particle-resolved simulations, which revealed the significant influence of heat transfer and particle's morphology on conversion rates (Zhang et al., 2024b, 2025a). At the reactor scale, computational fluid dynamics (CFD) frameworks have been utilized to connect process parameters, such as feeding methods, to product selectivity (Li et al., 2025). The study by Abdi et al. (Abdi et al., 2025) employed a CFD-DEM (discrete element method) approach to investigate radiative heat exchange between a high-temperature enclosure and moving layers of spherical particles, and demonstrated the dominant role of thermal radiation. Guiding these efforts, reviews have highlighted the potential of advanced methods like machine learning to refine kinetic predictions (Armenise, Wong, et al., 2021) and have outlined the progress and challenges in applying simulation to advance reactor design for plastic pyrolysis (Zhang, Li, et al., 2025).

While significant research has focused on the kinetics and product yields of plastic pyrolysis, the rate-limiting role of heat transfer remains poorly quantified. This is a critical gap, as thermal transport in large-scale, industrial reactors presents a significant challenge that often limits the overall process efficiency. This challenge is compounded by the strongly endothermic nature of the pyrolysis reaction, which actively opposes the heating process. Therefore, a fundamental understanding of the interplay between heat transfer and chemical reaction, which dictates the apparent reaction rate, is essential. This work bridges this gap by providing a direct, systematic, and quantitative analysis of this interplay. To achieve this, we developed a numerical model of a single plastic particle undergoing pyrolysis in a high-temperature environment. We then systematically varied key parameters (reactor temperature, particle diameter, and Nusselt number) to assess the competing dynamics of convective heat transfer and chemical reaction. From these results, we derived a quantitative correlation to predict pyrolysis time that captures the coupled thermo-chemical effects.

2. Simulation method

The numerical model is illustrated in Fig. 1. It simulates the pyrolysis of a plastic particle in a hot, inert nitrogen environment at a specified reactor temperature, T_R. The process begins as the particle absorbs heat from the surrounding gas via a convective heat flux, $\dot{Q}$. This heating increases the particle's temperature (T_p) until the onset of pyrolysis, at which point the particle's mass begins to decrease through the release of a volatile flux, $\dot{m}$.

The model assumes an idealized, spherical particle with an initial diameter of d_{p0}. This is physically justified because when heated, capillary forces drive the minimization of surface energy, causing irregular fragments and polymer foils to melt and retract into spherical droplets (Hejmady et al., 2021; Liedmann et al., 2017; Lotito & Zambelli, 2024). The particle is treated as homogeneous (0D), assuming intra-particle heat conduction is faster than external convective heat transfer and thus neglecting internal temperature gradients.

The numerical model is governed by a system of coupled ordinary differential equations (ODEs) representing the conservation of the particle's total mass and energy:

$$\frac{\mathrm{d}m_p}{\mathrm{d}t} = -k_r m_p^n m_{p0}^{1-n} \tag{1}$$

$$m_p c_{p,p} \frac{\mathrm{d}T_p}{\mathrm{d}t} = \dot{Q}_h - \dot{Q}_r \tag{2}$$

Eq. (1) follows the conversion-based framework of Bockhorn et al. (Bockhorn et al., 1999), but reformulates the mass balance directly in terms of the particle mass m_p, assuming a zero final mass (i.e., no char formation). m_{p0} denotes the initial particle mass. m_p decreases during pyrolysis while particle density is assumed constant, resulting in particle shrinkage over time. m_p is directly related to the particle diameter, d_p, by the geometric relationship $m_p = \frac{1}{6}\pi\rho_p d_p^3$.

A global kinetic model has been used to focus on heat transfer effects and overall conversion rather than detailed product distributions. The reaction was assumed as n-th order, and the rate coefficient, k_r, is calculated using the Arrhenius equation with a pre-exponential factor k_0, an activation energy E_a, and the universal gas constant R

$$k_r = k_0 \exp\left(-\frac{E_a}{RT_p}\right) \tag{3}$$

Heat is transferred to the particle from the hot surrounding atmosphere through the heating source

$$\dot{Q}_h = \alpha A_p (T_g - T_p), \quad \alpha = \frac{Nu \cdot \lambda_g}{d_p} \tag{4}$$

with the heat transfer coefficient α. Here, the gas thermal conductivity is denoted by λ_g, and the Nusselt number, Nu, is a prescribed input parameter rather than being calculated from empirical correlation. The energy balance includes a heat sink term, $\dot{Q}_r$, which accounts for the endothermic pyrolysis reaction and is calculated from the mass conversion rate and the heat of reaction, Δh_r

$$\dot{Q}_r = \dot{m}_p \Delta h_r \tag{5}$$

While the mass balance could be extended to include multiple reaction species, the primary focus of this work is to investigate the interaction between heat transfer and chemical kinetics on the overall pyrolysis conversion. Therefore, we have adopted a simplified, single-step reaction mechanism (*Plastics → Volatiles*) for modeling the pyrolysis process.

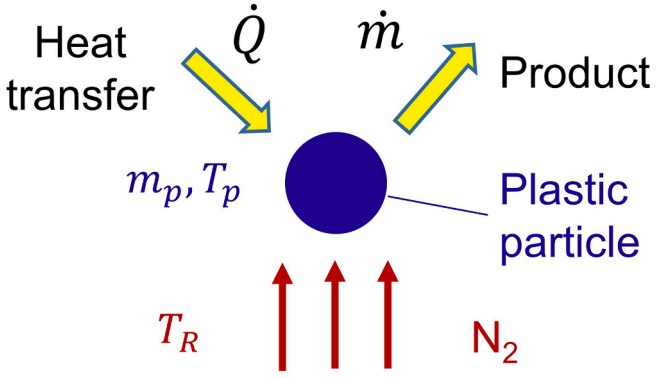

Fig. 1. Simulation setup for single-particle plastic pyrolysis.

The governing Eqs. (1) and (2) constitute a system of coupled, nonlinear ordinary differential equations (ODEs). These equations were solved using an in-house Python solver that couples the open-source Cantera library (Goodwin et al., 2021) to SciPy's VODE integrator for time integration (Virtanen et al., 2020). The VODE algorithm employs a variable-order, adaptive time-stepping scheme, making it particularly well-suited for the stiff initial value problems encountered in this study. It employs a backward differentiation formula (BDF) scheme with up to 5th-order accuracy. The integration is controlled by user-defined absolute and relative tolerances, which were both set to 1.5×10^{-8} s in this work.

3. Simulation setups

This study investigates the pyrolysis of five common plastics: low-density polyethylene (LDPE), high-density polyethylene (HDPE), polypropylene (PP), polystyrene (PS), and acrylonitrile butadiene styrene (ABS). The densities of different plastics (ρ_p) are given in Table 1, along with the thermal properties derived from our previous differential scanning calorimetry (DSC) measurements (Netsch et al., 2024). These properties include the melting (or glass transition) temperature (T_m^*), and melting enthalpy (h_f). The heat capacity, $c_{p,p}$, is implemented as a piecewise linear function of particle temperature, as shown in Eq. (6), with its coefficients also listed in the table. This piecewise approach accurately captures the distinct pre-melting, melting, and post-melting thermal regimes, with the latent heat of melting implicitly accounted for by a sharp increase in $c_{p,p}$ at the melting temperature. This increase in $c_{p,p}$ due to melting is considered over a particle temperature interval of $\Delta T = 4$ K around T_m^*, as shown Eq. (6). As detailed in (Netsch et al., 2024), amorphous polymers such as PS and ABS undergo a glass transition rather than a first order melting transition; they therefore lack a well defined melting point and enthalpy of fusion. Their thermal softening is represented via a temperature dependent specific heat capacity, which captures energy uptake during softening without the computational overhead of explicitly resolving a liquid phase. This treatment has been validated against pilot scale pyrolysis plant data and accurately reproduces the relevant thermal behavior (Netsch et al., 2024).

$$c_p(T_p) = \begin{cases} a_1 T_p + b_1, & T_p \le T_m^* - \dfrac{\Delta T}{2} \\ \dfrac{1}{2} h_f/\Delta T + a_1 T_p + b_1, & T_m^* - \dfrac{\Delta T}{2} < T_p < T_m^* \\ \dfrac{1}{2} h_f/\Delta T + a_2 T_p + b_2, & T_m^* \le T_p < T_m^* + \dfrac{\Delta T}{2} \\ a_2 T_p + b_2, & T_m^* + \dfrac{\Delta T}{2} \le T_p \end{cases} \quad (6)$$

The reaction kinetic parameters (k_0, E_a, n) for the rate law in Eq. (3) are listed in Table 2, which were derived from thermogravimetric (TG) experiments conducted at a constant heating rate (Netsch et al., 2025). The kinetic model and parameters were rigorously validated in our prior work using the root-mean-square deviation (RMSD) metric (Netsch et al., 2025), demonstrating high accuracy across all polymers. The apparent enthalpy of reaction (including enthalpy of evaporation), Δh_r, also listed in the table, was determined from DSC measurements (Netsch et al., 2024). The model ensures a consistent energy balance that includes the effects of heating, melting, and chemical reaction. A detailed description of the DSC methodology is provided in our previous work (Netsch et al., 2024). The surrounding nitrogen is modeled as an inert ideal gas with temperature-dependent properties (ρ_g, λ_g, and $c_{p,g}$) calculated with Cantera. All simulations were conducted at atmospheric pressure.

4. Results and discussions

4.1. Comparison with TG experiments

To demonstrate the validity of the proposed model, it was first used to simulate the TG experiments reported in our previous work (Netsch et al., 2025), covering heating rates (β) ranging from 2 to 40 °C/min. For each experiment, a 10 mg sample of a specific plastic (LDPE, HDPE, PP, PS, or ABS) was placed in a corundum crucible within a nitrogen atmosphere flowing at approximately 60 mL/min. The particle temperature was prescribed, which increases linearly from a starting temperature (T_0) of 40 °C to a maximum (T_{max}) of 900 °C, following the equation $T_p = T_0 + \beta \cdot t$. Consistent with the experimental setup, the numerical simulations used a particle mass of 10 mg and a prescribed particle temperature evolution.

Fig. 2 displays the simulated (solid lines) and experimental (dotted lines) conversion (X, top) and conversion rate (dX/dt, bottom) for LDPE, PP, and ABS versus particle temperature (T_p). Conversion is defined as the normalized mass loss

$$X = \frac{m_{p0} - m_p}{m_{p0}} \quad (7)$$

ranging from 0 (initial state) to 1 (complete pyrolysis). The model's validity is demonstrated by its strong agreement with measured data for the global degradation behavior of various plastics. The model accurately captures how pyrolysis shifts to higher temperatures at increased heating rates, which in turn accelerates the reaction. This phenomenon occurs because rapid heating minimizes the time spent at lower temperatures, shifting the bulk of the conversion to a higher-temperature regime where reaction kinetics are faster, thus confirming the critical role of the heating rate in the process. The discrepancies between model and experiments stem from the kinetic parameters of the global reaction model, which were fitted to TG data. The results for HDPE and PS exhibit comparable trends and accuracy, which were, therefore, omitted from Fig. 2 for visual clarity.

Table 2
Reaction kinetic parameters used for calculating the reaction rate.

Plastics	k_0[s^{-1}]	E_a [kJ/mol]	n [−]	Δh_r [kJ/kg]
HDPE	8.31×10^{16}	275	0.94	438
LDPE	3.80×10^{17}	281	0.94	473
PP	3.32×10^{14}	233	0.94	542
ABS	1.22×10^{14}	216	1.08	739
PS	6.37×10^{13}	209	0.94	744

Table 1
Physical parameters used for modeling plastic pyrolysis.

Plastic materials	ρ_p [kg/m^3]	T_m^* [°C]	a_1 [J/kg/K^2]	b_1 [J/kg/K]	a_2 [J/kg/K^2]	b_2 [J/kg/K]	h_f [kJ/kg]
HDPE	959	156	6.447	1674	3.250	2191	235
LDPE	919	125	4.376	2106	3.336	2238	142
PP	895	180	5.992	1636	3.095	2161	116
ABS	1110	100	3.695	1359	2.454	1796	-
PS	1060	105	5.308	1207	2.776	1668	-

4.2. Impact of heat transfer on pyrolysis conversion

Ideally, pyrolysis involves rapidly heating plastic particles to the target temperature so that decomposition proceeds at (or very near) the reactor temperature with minimal thermal lag. In practice, heating rates are limited by physical factors such as particle size and the prevailing heat transfer mechanism (e.g., gas–solid contact in a fluidized-bed reactor). To examine these realistic, heat-transfer-limited conditions, we simulate the pyrolysis of a plastic particle exposed to a hot convective environment. We conduct a parametric study for five plastics (LDPE, HDPE, PP, PS, and ABS), varying three key parameters: initial particle diameter ($d_{p0} = 2 - 4$ mm), Nusselt number ($Nu = 3 - 9$), and reactor temperature ($T_R = 470 - 530$ °C). The initial particle temperature is $T_{p0} = 25$ °C. The initial particle mass is determined from its size and material density. As detailed in Sec. 2, the particle is treated as stationary, and convective heat transfer is represented by prescribing *Nu*; the corresponding heat transfer coefficient used in the energy equation is obtained as shown in Eq. (4). This framework enables a systematic analysis of how convective heat transfer and reaction kinetics interact to control overall conversion across operating conditions.

The selected operating parameters reflect typical industrial conditions for plastic pyrolysis. In practice, pyrolysis is conducted between 400 and 600 °C, depending on the polymer type, reactor design, and target product distribution (Al-Salem et al., 2017; Lopez et al., 2017). For polyolefins targeting liquid-fuel production, temperatures of 450–550 °C are common: lower temperatures favor the formation of waxes and heavy oils, whereas higher temperatures promote light oils and gases. Comparable ranges apply to PS and PET. Industrial and pilot-scale fluidized bed reactors (FBRs) processing mixed polyolefin feeds often operate at approximately 480–520 °C to maximize liquid yield while minimizing excessive secondary cracking. Particle sizes were selected based on prior FBR pyrolysis studies of shredded plastic films (typically 2–5 mm) (Kaminsky & Kim, 1999; Predel & Kaminsky, 2000). This range corresponds to Geldart Group B hydrodynamics, ensuring stable fluidization and effective mixing, while facilitating rapid heating with minimal intra-particle thermal gradients for fast devolatilization. The chosen Nusselt number range is according to the work by Turton et al. (Turton et al., 1987), where measured values for *Nu* can reach up to 10 in FBRs. Under these operating conditions, the Biot number spans over $0.1 < Bi < 0.8$.

Using LDPE as a representative case, Fig. 3 illustrates, from left to right, the simulated evolution of particle temperature (T_p), conversion progress (X), reaction rate (dX/dt), and the profile of X versus T_p. A reference case ($d_{p0} = 3$ mm, $Nu = 6$ and $T_R = 500$ °C) is shown by the blue curves. To isolate the influence of each variable, one parameter was varied while the other two were held at their reference values. Fig. 3 reveals a distinct two-stage heating profile for the particle. First, T_p rises rapidly due to convection until pyrolysis initiates at around 450 °C. Thereafter, the heating rate slows dramatically, forming a temperature plateau. This occurs because the highly endothermic pyrolysis reaction counteracts the incoming heat flux. During the peak conversion period, the energy supplied by convection is almost entirely consumed by the reaction, causing the particle temperature to stagnate even as the ambient temperature remains high. This complex thermal behavior highlights that the process is governed by a dynamic competition between external heat transfer and the internal, endothermic reaction rate. A distinct plateau is observed in the particle's temperature profile around 112 °C, corresponding to the melting of LDPE. At this point, the heat supplied to the particle is consumed as latent heat (Table 1) rather than raising its temperature.

The operating parameters control the pyrolysis process by influencing the interplay between convective heat transfer and reaction kinetics. Limitations caused by convective heat transfer become apparent with a larger d_{p0} or a lower *Nu*. Both scenarios reduce the heat transfer coefficient due to $\alpha \propto Nu/d_p$, leading to slower heating and a smaller conversion rate. Consequently, the X vs. T_p profiles in Fig. 3 (last column) show that conditions favoring rapid heat transfer or kinetics (i. e., smaller d_{p0} and larger *Nu*) shift the main conversion stage to higher temperatures, accelerating the overall process. Conversely, a higher T_R accelerates the process primarily by enhancing reaction kinetics. While it does modestly increase the heating rate by enlarging the thermal driving force, its dominant effect is the exponential increase in the conversion rate according to the Arrhenius law. These trends, while only shown for LDPE, are representative and were observed for all other simulated plastics (HDPE, PP, PS, and ABS).

Fig. 4 illustrates the distinct pyrolysis behavior of different plastics under identical reference conditions: $d_{p0} = 3$ mm, $Nu = 6$ and $T_R = 500$ °C. Similar to the thermal behavior observed for LDPE in Fig. 3, all particles undergo rapid initial heating followed by a deceleration once the pyrolysis reaction begins. In the case of ABS and PS, the lower

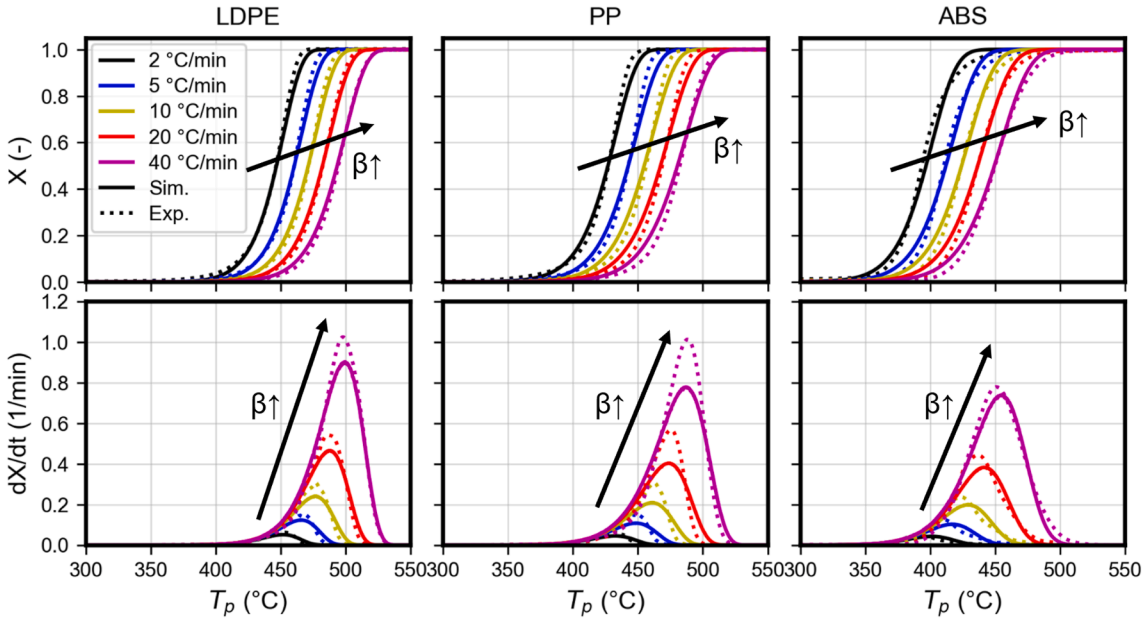

Fig. 2. Comparison of calculated (solid lines) and measured (dotted lines) conversion (top) and conversion rate (bottom) for LDPE, PP and ABS under different heating rates.

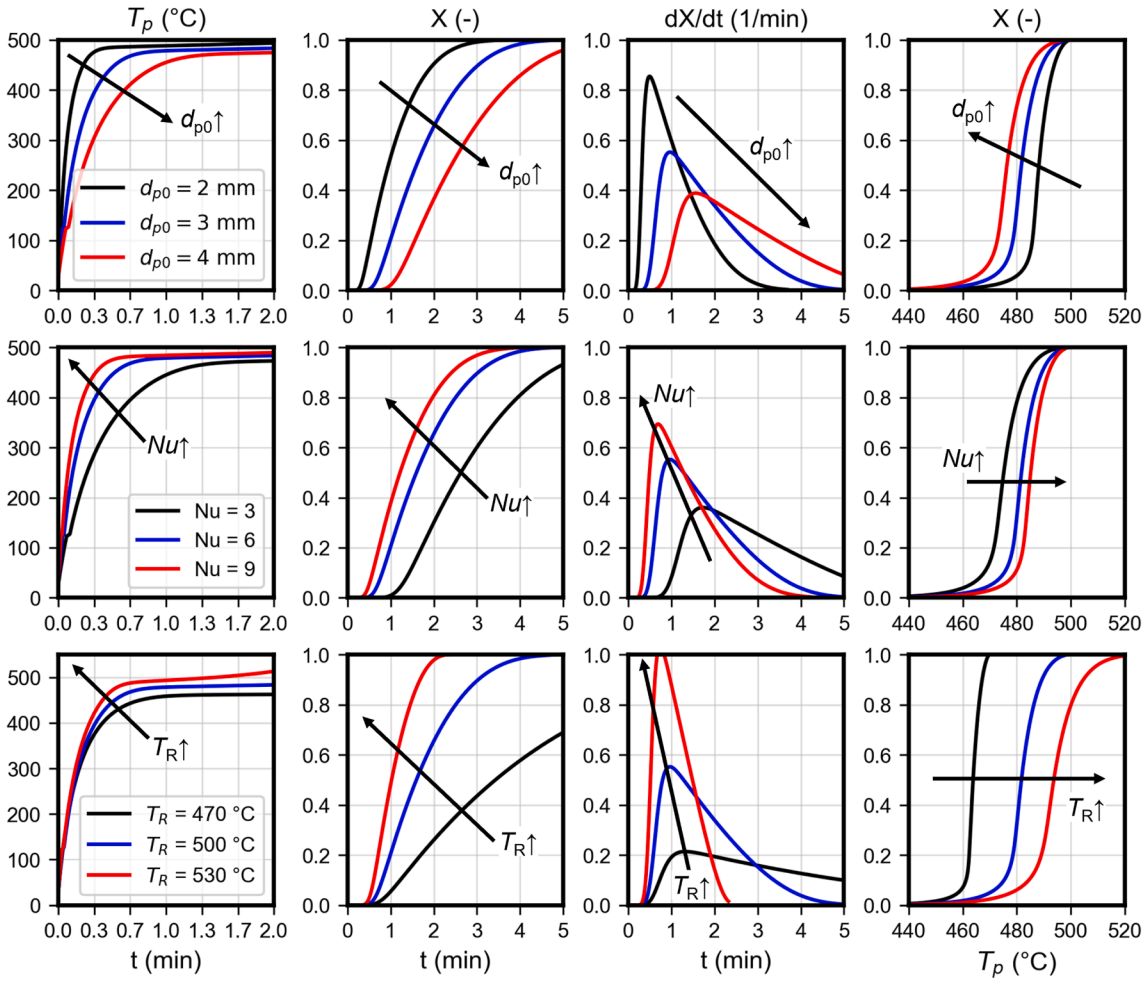

Fig. 3. Effect of varyning the initial particle diameter (top), the Nusselt number (middle), and the ambient temperature (bottom) on LDPE pyrolysis.

activation energy leads to an earlier onset of pyrolysis compared to the other plastics. It is worth noting that while our model assumes no char formation, Fig. 4(a) captures a clear temperature rise for ABS and PS near the end of conversion. This occurs as the external heat flux begins to dominate the effect of endothermic reaction. The overall reactivity follows a clear hierarchy: PS shows the fastest conversion and highest reaction rate, followed in descending order by ABS, PP, LDPE, and HDPE, as shown in Fig. 4(b and c). This order is reflected in the conversion temperature profiles (see Fig. 4(d)), where PS degrades at the lowest temperature range, confirming its higher reactivity.

Fig. 5 inspects the thermal behavior of different plastic particles by plotting the evolution of the primary heat source (the convective heating, $\dot{Q}_h$) and the primary heat sink (the endothermic reaction, $\dot{Q}_r$). The process is governed by a dynamic balance between these two terms. Initially, heat transfer dominates ($\dot{Q}_h \gg \dot{Q}_r = 0$), causing a rapid increase in particle temperature. As pyrolysis commences, $\dot{Q}_r$ grows, acting as a

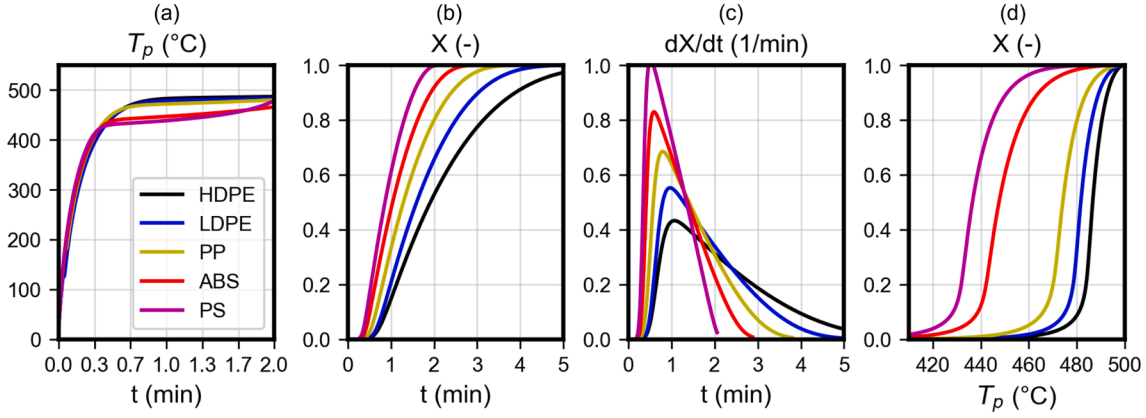

Fig. 4. Comparison of calculated time evolution of particle temperature (T_p), conversion (X), conversion rate (dX/dt) and correlation of X with T_p for different plastics.

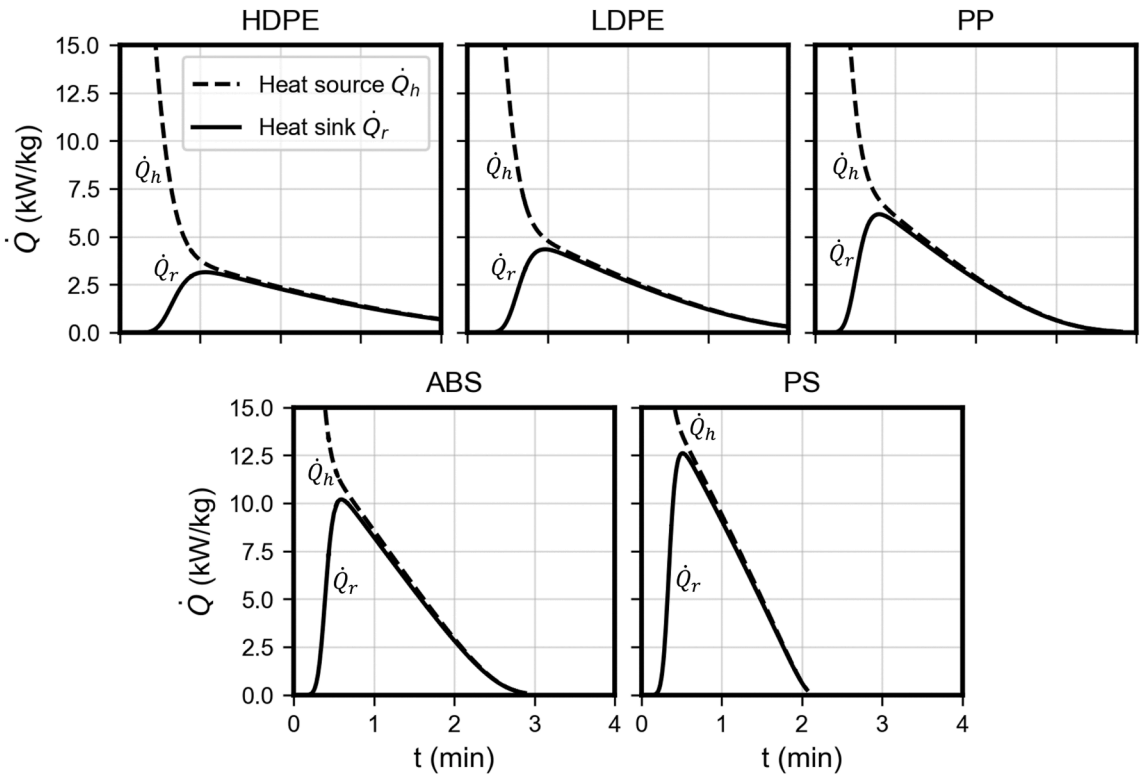

Fig. 5. Comparison of convective heating rate (Q_h, dashed) and endothermic reaction heat sink (Q_r, solid) from simulations of plastic pyrolysis for different polymer particles under identical operating conditions.

powerful heat sink that counteracts the external heating. During the peak reaction period, $\dot{Q}_r$ approaches the magnitude of $\dot{Q}_h$, resulting in a near-thermal-equilibrium where the particle temperature plateaus (as seen in Fig. 4(a)). Once the reaction subsides, both $\dot{Q}_r$ and $\dot{Q}_h$ diminish to 0. The interplay depends on the material. PS, in particular, exhibits the largest peak $\dot{Q}_r$, aligning with its higher reaction rate (Fig. 4(c)). This larger endothermic demand is also reflected in its total heat of reaction (the integral of $\dot{Q}_r$), which aligns with the values in Table 2. Ultimately, this competitive interplay between heat supply and consumption is the controlling mechanism for the entire conversion process.

4.3. Correlation of pyrolysis time with pyrolysis number

To quantify the interplay between the heating process and chemical kinetics, the dimensionless pyrolysis number (Py), defined as the ratio of the characteristic reaction time (t_c) to the characteristic heat transfer time (t_h), is widely utilized (Pyle & Zaror, 1984; Ruiz et al., 2023; Saade et al., 2015; Shotorban et al., 2005). In general, two distinct Pyrolysis numbers can be defined: one governing intra-particle heat transfer (Py_I) and another governing external convective heat transfer (Py_{II}). These two numbers are related via the Biot number (Bi) according to $Py_{II} = Bi \cdot Py_I$. Since intra-particle conduction is neglected in the current modeling, Py is defined here exclusively in terms of the convective heat transfer coefficient, α:

$$Py = \frac{t_c}{t_h} = \frac{\alpha}{k_r \rho_p c_{p,p} d_{p,0}} = \frac{Nu\lambda_g}{k_r \rho_p c_{p,p} d_{p0}^2} \tag{8}$$

In Eq. (8), the thermo-physical parameters (λ_g and $c_{p,p}$) and rate coefficient (k_r) in Eq. (8) are evaluated at the reactor temperature. Two distinct regimes are defined by the magnitude of Py. When $Py > 1$ (or $t_c > t_h$), the reaction is the slower, rate-limiting step. When $Py < 1$ or $t_c < t_h$, convective heat transfer becomes the bottleneck relative to the pyrolysis reaction. The operating parameters in this work yield $0.01 < Py < 52$, effectively spanning the transition between these two regimes. A shift towards the reaction-limited regime (high Py) occurs if heat transfer is enhanced or if the reaction slows. On the other hand, raising T_R drastically increases the reaction rate, leading to a lower Py and a transition toward heat-transfer control. Note that intra-particle heat conduction can become rate-limiting under certain conditions; this effect is not explicitly captured in the current model. A quantitative assessment of its impact is provided in Sec. 4.4. This use of a dimensionless number to compare process time scales is a well-established concept, similar to the role of the Damköhler number in fields like turbulent combustion (Zhang et al., 2017, 2022; Zhu et al., 2024; Zirwes et al., 2023).

To estimate the required pyrolysis time, extensive simulations were performed across the operating conditions: $2\ \text{mm} \le d_{p0} \le 4\ \text{mm}$, $3 \le Nu \le 9$ and $470\ ^\circ\text{C} \le T_R \le 530\ ^\circ\text{C}$. Fig. 6 shows the pyrolysis time (τ_{py}), defined as the time interval required for conversion from 1% to 99%, as a function of Py for different plastics. Note that the HDPE result at $T_R = 470\ ^\circ\text{C}$ is not visible in Fig. 6 because its τ_{py} is about 20 min, exceeding the figure's upper plotting limit used for cross-plastic comparison. The longer pyrolysis time required for HDPE compared to other plastics is a direct consequence of its inherently reaction kinetics. This is consistent with the slower conversion and lower reaction rates observed in Fig. 4(b and c). The results reveal that τ_{py} decreases with increasing T_R and exhibits an inverse relationship with Py at a constant T_R, delineating two distinct process regimes:

- **The reaction-kinetics limited regime ($Py > 1$):** in this regime, τ_{py} decreases only slowly and approaches an asymptote, becoming effectively independent of Py. The intrinsic chemical reaction is the slower, rate-limiting step, so further enhancements in convective heat transfer provide diminishing returns in accelerating pyrolysis.
- **The convective-heating limited regime ($Py \le 1$):** in this regime, convective heat transfer becomes important alongside the pyrolysis reaction, causing τ_{py} to decrease rapidly with increasing Py.

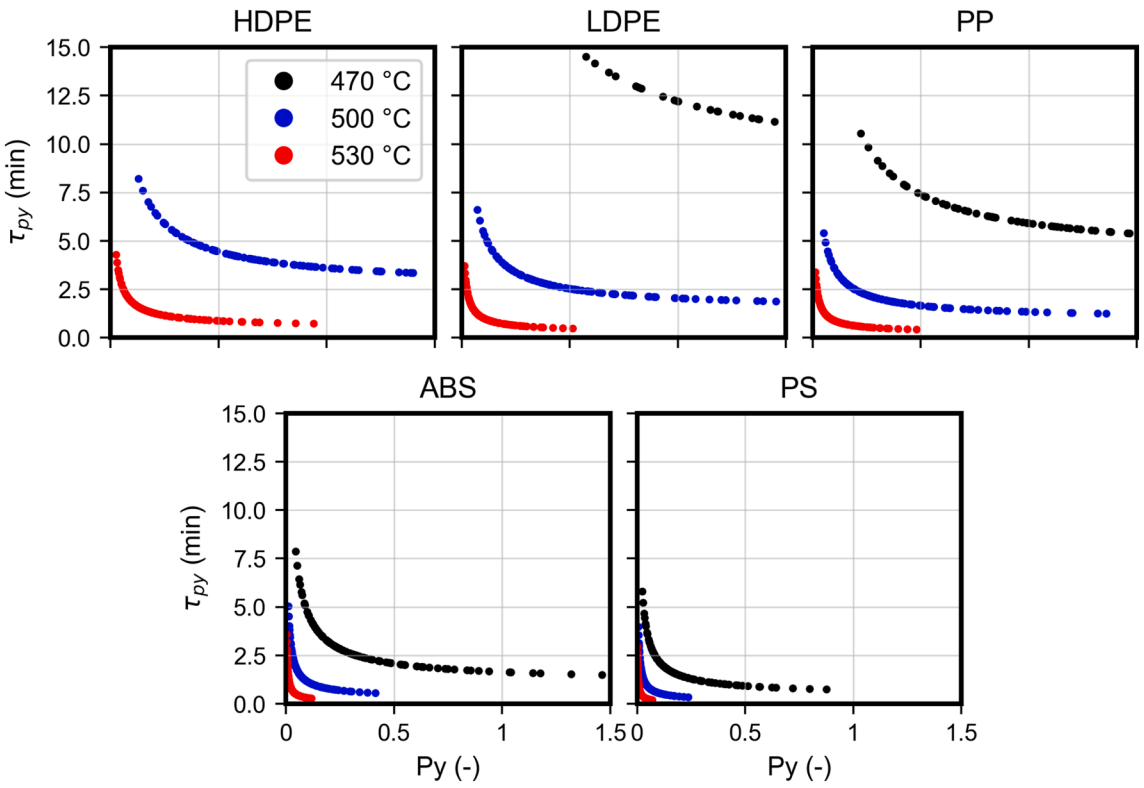

Fig. 6. Correlation between calculated pyrolysis time and pyrolysis number for various polymer types and operating conditions.

To convert the plastic particle at the desired reactor temperature, a fast-heating or reaction-limited regime ($Py > 1$) is preferred. At low heating rates ($Py < 1$), however, significant plastic conversion can occur at lower temperatures.

In Fig. 7, the pyrolysis time is normalized by the chemical time scale ($t_c = 1/k_r$) and plotted versus Py for all plastics and operating conditions considered. This normalization collapses the distinct curves observed at various T_R in Fig. 6 into a unified inverse correlation between τ_{py}/t_c and Py for each polymer. The result underscores the significant similarities for the competing interplay between pyrolysis reaction kinetics and heat transfer in governing the overall conversion rate. On the τ_{py}/t_c vs. Py plot, the data for HDPE, LDPE, and PP cluster closely, which is likely attributable to their shared chemical structure as polyolefins. The data pairs were fitted to the power law model presented in Eq. (9). The resulting fitted curves are depicted by solid lines in Fig. 7 individually for PE/PP, ABS and PS, along with the corresponding best-fit parameters compiled in Table 3.

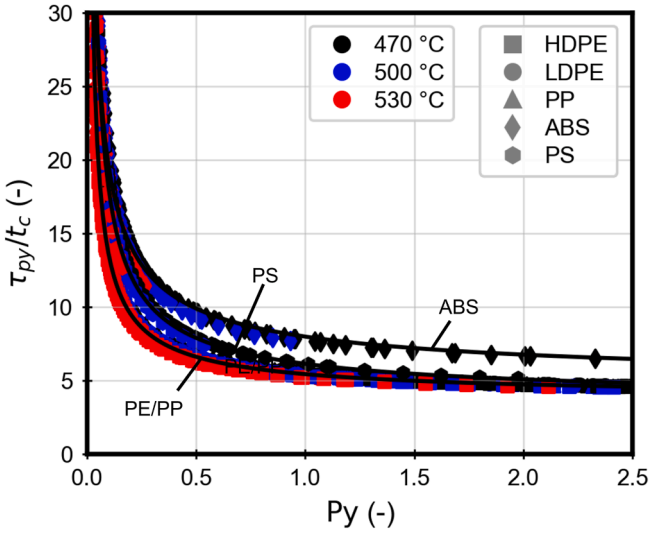

Fig. 7. Normalized pyrolysis time (τ_{py}/t_c) as a function of the Pyrolysis number (Py).

$$\frac{\tau_{py}}{t_c} = aPy^b + c \tag{9}$$

The analytical correlation presented in Eq. (9) can be used as an efficient tool for designing plastic pyrolysis processes, as it enables the prediction of the necessary feedstock residence time for specific operating conditions. The application is a two-step process. First, Py is evaluated with Eq. (8) based on the polymer type, particle size, reactor temperature, and Nusselt number. In the second step, this Py value is used to calculate τ_{py} using Eq. (9). To illustrate, for an LDPE particle with a 2 mm diameter at a reactor temperature of 450 °C and an average heating rate of 200 °C/min (corresponding to t_h = 2.25 min), the resulting Py is 3.8. Using Eq. (9), τ_{py} is calculated to be approximately 38 min, which is consistent with the value reported for LDPE in an auger-type reactor (Netsch et al., 2023), where after a residence time of 30 min, approximately 96 % of the polymer was converted to pyrolysis oil and gas. A primary challenge, however, is the difficulty in accurately assessing the heating rate for practical reactor designs.

Figs. 6 and 7 show that the pyrolysis time decreases drastically with increasing Py for $Py < 1$. This indicates that the reaction is enhanced by the higher temperatures achieved with faster heating. In contrast, for $Py > 1$, where the process becomes reaction-limited, a further increase in

Table 3
Fitting parameters used for Eq. (9) and Fig. 7.

Plastics	a	b	c
PE&PP	1.70	−0.76	3.75
PS	2.63	−0.74	3.52
ABS	3.42	−0.64	4.58

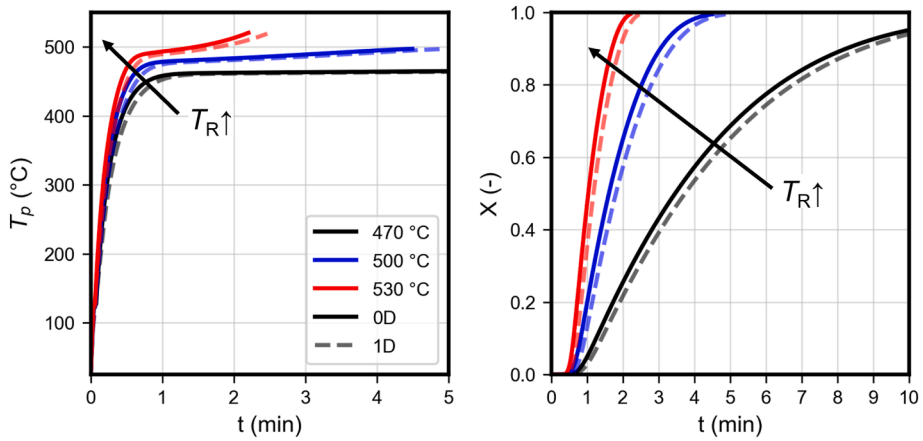

Fig. 8. Comparison of the simulated time evolution of particle temperature (left) and conversion progress (right) at different reactor temperatures, using both the homogeneous-particle model (solid line) and the particle-resolved model (dashed line).

the heating rate yields no significant acceleration. This indicates that near $Py \approx 1$, heat transfer and reaction rates are balanced, yielding near-ideal heating conditions in which conversion proceeds at the intended reactor temperature.

4.4. Impact of intra-particle heat conduction

Intra-particle heat conduction is a critical mechanism in plastic pyrolysis; given the low thermal conductivity of plastics, internal thermal resistance can significantly limit the overall conversion rate. However, this mechanism is neglected in the present 0D framework to reduce computational cost (consistent with other large-scale studies). To assess the validity of this assumption, particle-resolved simulations (1D, assuming spherical particles with axial symmetry) have been conducted that explicitly resolve internal temperature gradients. Fig. 8 compares the time histories of T_p and X for LDPE predicted by the original 0D model (solid) and the 1D benchmark (dashed) at $d_{p0} = 3$ mm, $Nu = 6$, and varying T_R. The results show that the 1D model, which accounts for finite intra-particle heat conduction, predicts slower heating and conversion. Although not shown, the discrepancy between the 0D and 1D models grows with increasing d_{p0}, T_R and Nu, consistent with a larger Bi. The largest deviation in T_p for LDPE occurs at the highest d_{p0}, T_R and Nu, corresponding to $Bi = 0.45$. In this case, the T_p error is about 2.7%, which lengthens the total conversion time τ_{py} by approximately 14.7%.

Given that particle-resolved simulations are significantly more computationally expensive than the homogeneous-particle model, applying them across the broad parameter space presented in Figs. 6 and 7 is infeasible. The comparison is therefore limited to LDPE to estimate the uncertainty arising from the assumption of negligible intra-particle heat conduction. Consequently, the correlation proposed in Eq. (9) likely underestimates τ_{py} due to the omission of internal heat transfer resistances. The magnitude of this deviation depends on Bi. A comprehensive quantitative assessment of this effect across all operating conditions and materials is beyond the scope of the present study and will be the subject of future work.

4.5. Discussions

The operating conditions examined here are representative of the local environments experienced by plastic particles in industrial systems. Efficient, uniform heating is a key challenge in these reactors and can lead to nonuniform temperatures and conversion. Our results show that this is most critical when heating is slow relative to the reaction rate ($Py < 1$): conversion then occurs below the reactor setpoint, adversely affecting product yields. Conversely, during slow pyrolysis (e.g., at low reactor temperatures), heat transfer becomes secondary and the process is kinetically limited ($Py > 1$).

While our model neglects the effects of particle geometry, melting, and internal conduction on the heat transfer process, the essential thermo-chemical interplay between heating and reaction kinetics remains robust. Crucially, the proposed analytical framework is adaptable, as these additional physical phenomena can be integrated by refining the characteristic time scale for heat transfer. Moreover, to test the robustness of our simplified reaction kinetic model, we also performed simulations (not detailed here) using the more complex, multi-step, lumped-reaction model proposed by Lechleitner et al. (2020). These results confirmed a similar thermo-chemical interplay, strengthening the results drawn from our primary analysis.

5. Conclusion

This study employs numerical simulations to investigate the influence of convective heat transfer on chemical reactions during the pyrolysis of a plastic particle. To explore the interplay between thermal and chemical effects, various scenarios were simulated by altering the most important parameters, the particle size, the heat transfer coefficient and the reactor temperature. The interplay between these processes was quantified using the pyrolysis number (Py), which is defined as the ratio of the characteristic time scale of the chemical reaction to that of the convective heat transfer. The principal findings of this study are as follows:

- The pyrolysis process is governed by the interplay between external heat transfer and the endothermic reaction. These mechanisms balance each other, resulting in conversion at a near-constant temperature.
- Pyrolysis time τ_{py} exhibits a strong inverse correlation with Py, which is valid for all plastic materials investigated.
- A quantitative correlation is developed to predict τ_{py} from Py for various plastics, demonstrating validity over a wide range of operating conditions.
- Finite intra-particle heat conduction slows both heating and pyrolysis, extending τ_{py} by up to 15% for LDPE under the conditions investigated.

The analysis in this study was based on a simplified model, assuming a spherical, thermally thin particle and a single-step reaction mechanism. Future work will therefore focus on expanding this framework to broader scenarios by considering the effects of non-ideal, thermally thick particles for different plastic materials, incorporating phase transitions like melting, and employing more detailed reaction kinetic models.

CRediT authorship contribution statement

Feichi Zhang: Writing – review & editing, Writing – original draft, Visualization, Methodology, Investigation, Formal analysis, Conceptualization. **Muhao Li:** Writing – review & editing, Software, Methodology. **Xiaoyue Ma:** Visualization, Resources, Conceptualization. **Niklas Netsch:** Writing – review & editing, Data curation. **Salar Tavakkol:** Writing – review & editing, Supervision, Project administration, Funding acquisition. **Thorsten Zirwes:** Writing – review & editing, Software, Methodology. **Rui Zhang:** Writing – review & editing. **Dieter Stapf:** Supervision, Project administration, Funding acquisition.

Declaration of competing interest

The authors declare that they have no known competing financial interests or personal relationships that could have appeared to influence the work reported in this paper.

Acknowledgments

The authors gratefully acknowledge the financial support by the Helmholtz Association of German Research Centers (HGF), within the research program Materials and Technologies for the Energy Transition (MTET), topic Resource and Energy Efficiency.

References

Abdi, R., Jaeger, B., Illana, E., Wirtz, S., Schiemann, M., & Scherer, V. (2025). Modelling of heat transfer in moving granular assemblies with a focus on radiation using the discrete ordinate method: A dem-cfd approach. *Particuology, 100*, 78–94.

Al-Salem, S. M., Antelava, A., Constantinou, A., Manos, G., & Dutta, A. (2017). A review on thermal and catalytic pyrolysis of plastic solid waste (psw). *Journal of Environmental Management, 197*, 177–198.

Armenise, S., SyieLuing, W., Ramírez-Velásquez, J. M., Launay, F., Wuebben, D., Ngadi, N., Rams, J., & Muñoz, M. (2021). Plastic waste recycling via pyrolysis: A bibliometric survey and literature review. *Journal of Analytical and Applied Pyrolysis, 158*(9).

Armenise, S., Wong, S., Ramírez-Velásquez, J. M., Launay, F., Wuebben, D., Nyakuma, B. B., Rams, J., & Muñoz, M. (2021). Application of computational approach in plastic pyrolysis kinetic modelling: A review. *Reaction Kinetics, Mechanisms and Catalysis, 134*(2), 591–614.

Bockhorn, H., Hornung, A., & Hornung, U. (1999). Mechanisms and kinetics of thermal decomposition of plastics from isothermal and dynamic measurements. *Journal of Analytical and Applied Pyrolysis, 50*(2), 77–101.

Ceamanos, J., Mastral, J. F., Millera, A., & Aldea, M. (2002). Kinetics of pyrolysis of high density polyethylene. comparison of isothermal and dynamic experiments. *Journal of Analytical and Applied Pyrolysis, 65*(2), 93–110.

Cheng, L., Gu, J., Wang, Y., Zhang, J., Yuan, H., & Chen, Y. (2020). Polyethylene high-pressure pyrolysis: Better product distribution and process mechanism analysis. *Chemical Engineering Journal, 385*, Article 123866.

Das, P., & Tiwari, P. (2017). Thermal degradation kinetics of plastics and model selection. *Thermochimica Acta, 654*, 191–202.

Geyer, R., Jambeck, J. R., & Law, K. L. (2017). Production, use, and fate of all plastics ever made. *Science Advances, 3*, Article e1700782.

Goodwin, D. G., Speth, R. L., Moffat, H. K., & Weber, B. W. (2021). *Cantera: An object-oriented software toolkit for chemical kinetics, thermodynamics, and transport processes*.

Hejmady, P., van Breemen, L. C. A., Anderson, P. D., & Cardinaels, R. (2021). A processing route to spherical polymer particles via controlled droplet retraction. *Powder Technology, 388*, 401–411.

Kaminsky, W. (2021). Chemical recycling of plastics by fluidized bed pyrolysis. *Fuel Communications, 8*, Article 100023.

Kaminsky, W., & Kim, J. (1999). Pyrolysis of mixed plastics for recovering chemical energy and feedstocks. *Energy & Fuels, 13*(1), 125–131.

Kusenberg, M., Eschenbacher, A., Djokic, M. R., Zayoud, A., Ragaert, K., De Meester, S., & Van Geem, K. M. (2022). Opportunities and challenges for the application of post-consumer plastic waste pyrolysis oils as steam cracker feedstocks: To decontaminate or not to decontaminate? *Waste Management (Tucson, Arizona), 138*, 83–115.

Lechleitner, A. E., Schubert, T., Hofer, W., & Lehner, M. (2020). Lumped kinetic modeling of polypropylene and polyethylene co-pyrolysis in tubular reactors. *Processes, 9*(1), 34.

Li, M., Zhang, F., Tavakkol, S., Zirwes, T., Stein, O. T., & Stapf, D. (2025). Simulation of plastics pyrolysis in fluidized bed with a lumped reaction kinetic model. In *2nd international workshop on reacting particle-gas systems: Modelling and experimental characterization of reactive particle-gas systems* (pp. 97–100). Magdeburg.

Liedmann, B., Arnold, W., Krüger, B., Becker, A., Krusch, S., Wirtz, S., & Scherer, V. (2017). An approach to model the thermal conversion and flight behaviour of refuse derived fuel. *Fuel, 200*, 252–271.

Lopez, G., Artetxe, M., Amutio, M., Bilbao, J., & Olazar, M. (2017). Thermochemical routes for the valorization of waste polyolefinic plastics to produce fuels and chemicals. A review. *Renewable and Sustainable Energy Reviews, 73*, 346–368.

López, A., De Marco, I., Caballero, B. M., Laresgoiti, M. F., & Adrados, A. (2011). Influence of time and temperature on pyrolysis of plastic wastes in a semi-batch reactor. *Chemical Engineering Journal, 173*(1), 62–71.

Lotito, V., & Zambelli, T. (2024). Heat: A powerful tool for colloidal particle shaping. *Advances in Colloid and Interface Science, 331*, Article 103240.

Mazloum, S., Aboumsallem, Y., Awad, S., Allam, N., & Loubar, K. (2021). Modelling pyrolysis process for pp and hdpe inside thermogravimetric analyzer coupled with differential scanning calorimeter. *International Journal of Heat and Mass Transfer, 176*, Article 121468.

Mazloum, S., Awad, S., Allam, N., Aboumsallem, Y., Loubar, K., & Tazerout, M. (2021). Modelling plastic heating and melting in a semi-batch pyrolysis reactor. *Applied Energy, 283*, Article 116375.

Netsch, N., Schröder, L., Zeller, M., Neugber, I., Merz, D., Klein, C. O., Tavakkol, S., & Stapf, D. (2025). Thermogravimetric study on thermal degradation kinetics and polymer interactions in mixed thermoplastics. *Journal of Thermal Analysis and Calorimetry, 150*(1), 211–229.

Netsch, N., Vogt, J., Richter, F., Straczewski, G., Mannebach, G., Fraaije, V., Tavakkol, S., Mihan, S., & Stapf, D. (2023). Chemical recycling of polyolefinic waste to light olefins by catalytic pyrolysis. *Chemie Ingenieur Technik, 95*(8), 1305–1313.

Netsch, N., Zeller, M., Richter, F., Bergfeldt, B., Tavakkol, S., & Stapf, D. (2024). Energy demand for pyrolysis of mixed thermoplastics and waste plastics in chemical recycling: Model prediction and pilot-scale validation. *ACS SRM, 1*(7), 1485–1492.

Predel, M., & Kaminsky, W. (2000). Pyrolysis of mixed plastics in a fluidized-bed reactor. *Polymer Recycle, 6*(1), 27–36.

Pyle, D. L., & Zaror, C. A. (1984). Heat transfer and kinetics in the low temperature pyrolysis of solids. *Chemical Engineering Science, 39*(1), 147–158.

Ragaert, K., Delva, L., & Van Geem, K. (2017). Mechanical and chemical recycling of solid plastic waste. *Waste Management (Tucson, Arizona), 69*(8), 24–58.

Ruiz, M. P., Zairin, D. M., & Kersten, S. R. A. (2023). On the intrinsic reaction rate of polyethylene pyrolysis and its interplay with mass transfer. *Chemical Engineering Journal, 469*, Article 143886.

Saade, R., Fard, M., Moghtaderi, B., & Page, A. C. (2015). A critical review of thermal decomposition and reaction front propagation in solid fuels. *Progress in Energy and Combustion Science, 47*, 1–32.

Shotorban, B., Klingenberg, D. J., & Baird, D. G. (2005). Heat transfer and reaction in single-particle polymer pyrolysis. *Polymer Engineering & Science, 45*(12), 1644–1654.

Silvarrey, D., & Phan, A. (2016). Kinetic study of municipal plastic waste. *International Journal of Hydrogen Energy, 41*(37), 16352–16364.

Singh, R. K., Ruj, B., Sadhukhan, A. K., & Gupta, P. (2019). Impact of fast and slow pyrolysis on the degradation of mixed plastic waste: Product yield analysis and their characterization. *Journal of the Energy Institute, 92*(6), 1647–1657.

Turton, R., Colakyan, M., & Levenspiel, O. (1987). Heat transfer from fluidized beds to immersed fine wires. *Powder Technology, 53*(3), 195–203.

Virtanen, P., Gommers, R., Oliphant, T. E., Haberland, M., Reddy, T., Cournapeau, D., Burovski, E., Peterson, P., Weckesser, W., Bright, J., et al. (2020). Scipy 1.0: Fundamental algorithms for scientific computing in python. *Nature Methods, 17*(3), 261–272.

Wang, J., Ma, Y., Li, S., & Yue, C. (2023). Study of hdpe plastic pyrolysis characteristics using high pressure autoclave. *Journal of the Energy Institute, 108*, Article 101244.

Zeller, M., Garbev, K., Weigel, L., Saatzer, T., Merz, D., Tavakkol, S., & Stapf, D. (2023). Thermogravimetric studies, kinetic modeling and product analysis of the pyrolysis of model polymers for technical polyurethane applications. *Journal of Analytical and Applied Pyrolysis, 171*, Article 105976.

Zhang, F., Cao, J., Zirwes, T., Netsch, N., Tavakkol, S., Zhang, R., Bockhorn, H., & Stapf, D. (2024). Numerical simulation of thermal decomposition of polyethylene with a single-particle model. In A. C. Benim, R. Bennacer, A. A. Mohamad, P. Ocłoń, S.-H. Suh, & J. Taler (Eds.), *Advances in computational heat and mass transfer* (pp. 180–191). Cham: Springer International Publishing.

Zhang, F., Li, M., Tavakkol, S., Zirwes, T., & Stapf, D. (2025). Modeling of plastic pyrolysis. In *2nd international workshop on reacting particle-gas systems: Modelling and experimental characterization of reactive particle-gas systems* (pp. 65–68). Magdeburg.

Zhang, F., Tavakkol, S., Dercho, S., Zhou, J., Zirwes, T., Zeller, M., Vogt, J., Zhang, R., Bockhorn, H., & Stapf, D. (2024). Assessment of dynamic characteristics of fluidized beds via numerical simulations. *Physics of Fluids, 36*(2), Article 023348.

Zhang, F., Tavakkol, S., Galeazzo, F. C., & Stapf, D. (2025). Particle-resolved simulation of the pyrolysis process of a single plastic particle. *Heat and Mass Transfer, 61*(1), 12.

Zhang, F., Zirwes, T., Habisreuther, P., & Bockhorn, H. (2017). Effect of unsteady stretching on the flame local dynamics. *Combustion and Flame, 175*, 170–179.

Zhang, F., Zirwes, T., Wang, Y., Chen, Z., Bockhorn, H., Trimis, D., & Stapf, D. (2022). Dynamics of premixed hydrogen/air flames in unsteady flow. *Physics of Fluids, 34*(8), Article 08512.

Zhu, J., Zirwes, T., Zhang, F. C., Li, Z. J., Zhang, Y., & Pan, J. F. (2024). Correlation of wall heat loss with quenching distance for premixed h2/air flames during unsteady flame-wall interaction. *Chemical Engineering Science, 283*, Article 119391.

Zirwes, T., Zhang, F., & Bockhorn, H. (2023). Memory effects of local flame dynamics in turbulent premixed flames. *Proceedings of the Combustion Institute, 39*(2), 2349–2358.